DRAFT VERSION MARCH 25, 2014
Preprint typeset using LaTeX style emulateapj v. 04/17/13

arXiv:1403.5872v1 [astro-ph.HE] 24 Mar 2014

DUST FORMATION IN MACRONOVAE

HAJIME TAKAMI[1,4], TAKAYA NOZAWA[2], KUNIHITO IOKA[1,3]

Draft version March 25, 2014

ABSTRACT

We examine dust formation in macronovae (as known as kilonovae), which are the bright ejecta of neutron star binary mergers and one of the leading sites of r-process nucleosynthesis. We find that dust grains of r-process elements are difficult to form because of the low number density of the r-process atoms even with their high abundances, while carbon or elements lighter than irons can condense into dust if they are abundant. Dust grains absorb emission from ejecta with opacity even greater than that of the r-process elements, and re-emit photons in infrared bands. Such dust emission can potentially account for the first macronova candidate associated with GRB 130603B, and pose an alternative model without r-process nucleosynthesis in macronovae. This dust scenario predicts a more featureless spectrum than the r-process model and day-scale optical-to-ultraviolet emission.

Keywords: binaries: general — dust, extinction — gamma-ray burst: individual (GRB 130603B) — infrared: stars — methods: numerical — stars: neutron

1. INTRODUCTION

The mergers of compact star binaries are the most promising astrophysical phenomena for the direct detection of gravitational waves (GWs) by the next generation GW interferometers, such as advanced LIGO (Abadie & LIGO Collaboration 2010), advanced VIRGO (Accadia et al. 2011), and KAGRA (Kuroda & LCGT Collaboration 2010). The detection of GWs enables us to test general relativity and to understand the nature of neutron stars (NSs), such as the equation of state.

Follow-up detection of electromagnetic (EM) counterparts of GW sources plays a complementary role to the GW detection. Only the detection of GWs is difficult to determine the position of GW sources accurately; typical localization uncertainty is ~ 10 - 100 deg^2 (e.g., LIGO Scientific Collaboration et al. 2013). The detection of EM counterparts helps localization, and can maximize scientific returns from a GW detection.

Recent numerical simulations have revealed that the mergers of neutron star binaries (NSBs), i.e., NS-NS binaries and black hole (BH)-NS binaries, eject significant mass ($\sim 10^{-4}M_\odot - 10^{-2}M_\odot$) dynamically (e.g., Rosswog et al. 1999; Ruffert & Janka 2001; Hotokezaka et al. 2013a; Bauswein et al. 2013; Kyutoku et al. 2013) and/or by neutrino-driven (e.g., Ruffert et al. 1997; Rosswog et al. 2003; Dessart et al. 2009; Metzger & Fernández 2014) or magnetically driven winds (e.g., Shibata et al. 2011). Emission from the ejecta by radioactive heating serves as a promising EM counterpart (Li & Paczyński 1998; Kulkarni 2005; Metzger et al. 2010; Barnes & Kasen 2013; Tanaka & Hotokezaka 2013; Tanaka et al. 2014). The ejecta also interact with circumsteller matter and radiate similarly to supernova remnants (Nakar & Piran 2011; Piran et al. 2013; Takami et al. 2013; Kyutoku et al. 2014).

In the ejecta of NSB mergers, different types of nucleosynthesis may take place, depending on the electron fraction Y_e. The ejecta can be neutron-rich (low Y_e), in which the r-process nucleosynthesis occurs efficiently (e.g., Goriely et al. 2011; Korobkin et al. 2012; Bauswein et al. 2013). In this case, the r-process elements, especially lanthanoids, provide large opacity for ejecta ($\kappa \sim 10$ cm^2 s^{-1}; Barnes & Kasen 2013; Tanaka & Hotokezaka 2013, called the r-process model), so that their luminosity peaks at late time ~ 10 days, compared with the original model without the r-process nucleosynthesis (~ 1 day with $\kappa \sim 0.1$ cm^2 s^{-1}; Li & Paczyński 1998; Metzger et al. 2010). The r-process model successfully reproduces the near-infrared (NIR) brightening in the afterglow of short gamma-ray burst (GRB) 130603B ($z = 0.356$; Berger et al. 2013; Tanvir et al. 2013; Hotokezaka et al. 2013b), which is called a macronova[5]. Here, the r-process elements also power emission through radioactive decay products. On the other hand, relatively high Y_e ($\sim 0.2 - 0.5$) can be also realized, which have been exclusively discussed for neutrino-driven winds (e.g., Fernández & Metzger 2013; Rosswog et al. 2013; Surman et al. 2013; Metzger & Fernández 2014, see also Wanajo et al. (2014) for locally low Y_e dynamical ejecta). In such environments, r-process nucleosynthesis is inefficient, but heavy elements (up to ^{56}Ni) may be synthesized from the constituent nucleons of NS matter, e.g., through a series of captures of α particles by ^{12}C produced from the triple-α process (e.g., Surman et al. 2013).

In this Letter, we investigate dust formation in the ejecta of NSB mergers for the first time. The formation of dust in macronovae is expected as in supernovae (e.g., Nozawa et al. 2003) because heavy elements may be synthesized and the temperature of ejecta inferred from GRB 130603B is low enough for dust formation. Then, we discuss that the newly formed dust can be responsible for the opacity of ejecta and that its emission can potentially reproduce the NIR excess of GRB 130603B. Although the r-process model can consistently explain this macronova, it is based on the limited observational data. Thus, it is worth considering another scenario (e.g., see Jin et al. (2013)).

[1] Institute of Particle and Nuclear Studies, KEK, 1-1, Oho, Tsukuba 305-0801, Japan; e-mail: takami@post.kek.jp, kunihito.ioka@kek.jp
[2] Kavli Institute for the Physics and Mathematics of the Universe, the University of Tokyo, 5-1-5, Kashiwanoha, Kashiwa, Chiba 277-8583, Japan; takaya.nozawa@ipmu.jp
[3] Department of Particle and Nuclear Physics, the Graduate University for Advanced Studies, Tsukuba 305-0801, Japan
[4] JSPS Research Fellow

[5] In this Letter, the word of macronovae means brightening following NSB mergers at an early epoch, not specifying radioactivity-powered emission.

2. PARAMETER ESTIMATION

Dust formation depends on the time evolution of gas density and temperature. We assume uniform ejecta with temperature T and density ρ for simplicity. The NIR macronova of GRB 130603B gives only one observational point (Tanvir et al. 2013): the absolute AB J-band magnitude of $M(J)_{\rm AB} = -15.35$ at $t \sim 7$ days after GRB 130603B in the rest frame. At this time, ejecta are likely in a free expansion phase, and the radius of the ejecta is

$$R = 3.6 \times 10^{15} \left(\frac{\beta}{0.2}\right) \left(\frac{t}{7\ \rm days}\right) \quad \rm cm, \tag{1}$$

where β is the ejecta speed in the unit of light speed c. The value of β is basically determined by the escape velocity of NSs. Throughout this Letter, $\beta = 0.2$ is adopted.

We can estimate the temperature of the ejecta at $t_0 = 7$ days from the luminosity as $T_0 \sim 2000$ K. Then, the temporal evolution of T is

$$T = T_0 \left(\frac{t}{7\ \rm days}\right)^{-s}. \tag{2}$$

where $s = 1$ for adiabatic expansion and $s = (\alpha+2)/4$ for the case with the heating rate $\propto t^{-\alpha}$. The latter relation can be derived from the second law of thermodynamics, $Td(T^3R^3)/dt \propto t^{-\alpha}$ (Li & Paczyński 1998). Recent detailed studies of r-process nucleosynthesis have suggested $\alpha = 1.2$ - 1.3 (Metzger et al. 2010; Korobkin et al. 2012; Rosswog et al. 2013; Wanajo et al. 2014). Our results are not sensitive to s because the temperature at which dust grains are formed is not far from T_0.

The density of the ejecta ρ_0 at $t = t_0$ is estimated from the condition that the diffusion time of photons in the ejecta $\sim \rho_0 R^2 \kappa / c$ is comparable with the dynamical time $\sim R/c\beta$ for a given opacity coefficient κ. The upper limit of the NIR flux at ~ 20 days in the rest frame suggests that the luminosity peaks at ~ 10 days (Tanvir et al. 2013). The density scales as $\rho = \rho_0 (t/t_0)^{-3}$ and therefore,

$$\rho \sim 1.4 \times 10^{-16} \left(\frac{\kappa}{10\ \rm cm^2 g^{-1}}\right)^{-1} \left(\frac{\beta}{0.2}\right)^{-2} \left(\frac{t}{7\ \rm days}\right)^{-3} \ \rm g\ cm^{-3}. \tag{3}$$

We examine the following two cases for ejecta density. One is low-density ejecta with $\kappa = 10$ cm^2 g^{-1}. This corresponds to the case that r-process elements are efficiently synthesized and are responsible for the opacity of the gas (Kasen et al. 2013; Tanaka & Hotokezaka 2013). The other is high-density ejecta with $\kappa = 0.1$ cm^2 g^{-1}, which corresponds to the opacity coefficient of Fe-rich Type Ia supernovae (e.g., Pinto & Eastman 2000), i.e., the case that r-process nucleosynthesis is inefficient.

The corresponding mass of the ejecta $M = \Delta\Omega R^3 \rho/3$ is

$$M \sim 1.4 \times 10^{-2} M_\odot \left(\frac{\Delta\Omega}{4\pi}\right) \left(\frac{\kappa}{10\ \rm cm^2 g^{-1}}\right)^{-1} \left(\frac{\beta}{0.2}\right), \tag{4}$$

where $\Delta\Omega$ is the solid angle with which the ejecta are blown off. Regarding dynamical ejecta, recent general relativistic hydrodynamical simulations have indicated $\Delta\Omega/4\pi \sim 1$ for NS-NS mergers (Hotokezaka et al. 2013a), and $\Delta\Omega/4\pi \sim 0.1$ for BH-NS mergers (Kyutoku et al. 2013).

3. DUST FORMATION

3.1. *Dust formation in the ejecta*

Dust can form below the equilibrium temperature at which the partial pressure of a focused element i equals to the vapor pressure of the condensate which depends only on temperature and atomic species. Partial gas pressure can be calculated from T and $\rho_i = f_i \rho$ with the equation of state of ideal gas, where f_i is the mass fraction of the element i. This study focuses on several representative elements individually instead of considering complicated composition to avoid complexity. The elements considered are listed in Table 1; Sr and Pt correspond to elements in the first and third peaks of the r-process nucleosynthesis, respectively. Hf is taken as a substitution of lanthanoid elements[6].

One of the conditions necessary for dust formation is that the timescale of collisions between atoms $\tau_{\rm coll} = [\pi a_0^2 n_i \langle v \rangle]^{-1}$ is much shorter than the timescale of the expansion of the ejecta $\tau_{\rm exp} = |(1/\rho)(d\rho/dt)|^{-1}$. Here, $a_0 \sim 1$ Å, $n_i = \rho_i/m_i$, and m_i are the radius, number density, and mass of the atom of a given element i. The mean thermal velocity is represented by $\langle v \rangle = (2k_{\rm B}T/m_i)^{1/2}$ and the mass of the atom is $m_i = A_i m_{\rm H}$, where $k_{\rm B}$ is the Boltzmann constant, $m_{\rm H}$ is the mass of a hydrogen atom, and A_i is the molecular weight of the element i. Then, using equations (2) and (3), the ratio $\tau_{\rm coll}/\tau_{\rm exp}$is

$$\begin{aligned} \frac{\tau_{\rm coll}}{\tau_{\rm exp}} &= \frac{3A_i m_{\rm H}}{\pi a_0^2 f_i \rho_0 t_0} \left(\frac{A_i m_{\rm H}}{2k_{\rm B}T_0}\right)^{1/2} \left(\frac{T}{T_0}\right)^{-\frac{2}{s}-\frac{1}{2}} \\ &\simeq 0.32 f_{\rm i}^{-1} \left(\frac{A_i}{100}\right)^{\frac{3}{2}} \left(\frac{\rho_0}{1.4\times10^{-16}\ \rm g\ cm^{-3}}\right)^{-1} \\ &\quad \times \left(\frac{T}{2000\ \rm K}\right)^{-\frac{2}{s}-\frac{1}{2}}. \end{aligned} \tag{5}$$

This ratio is sensitive to the temperature ($\propto T^{-3.0}$ for $\alpha = 1.2$), and increases with time. The formation of a dust grain is impossible if this ratio is above unity. For instance, the ratio is ~ 1 in the low density ejecta with $f_i \sim 0.5$ and $A_i \sim 200$, which indicates that dust grains of r-process elements are difficult to form.

Dust formation can be calculated with T and ρ given in the previous section and given composition. We calculate dust formation by applying the formulation of non-steady-state dust formation in Nozawa & Kozasa (2013) with $s = 0.8$, i.e., $\alpha = 1.2$.

The results of dust formation calculations are summarized in Figure 1. In the low-density ejecta with efficient r-process nucleosynthesis ($\kappa = 10$ cm^2 g^{-1}), Sr, Hf, and Pt never condense into dust grains even for $f_i = 1$. Here, dust grains are defined as clusters containing atoms more than a hundred. Fe grains ($A_i = 56$) cannot be also formed even if $f_i = 0.5$ because of its low condensation temperature ($\lesssim 1000$ K). Note that condensation temperature is lower than the equilibrium temperature because supersaturation is required for dust formation. The formation of carbon grains is possible as a result of the high condensation temperature ($\gtrsim 1800$ K) and small molecular weight ($A_i = 12$; see Equation 5), i.e., large number density. Their condensation efficiency is $f_{\rm con} = 0.08$ for $f_i = 0.5$. These carbon grains could be responsible for the opacity of ejecta if a significant amount of carbon exists even

[6] The data necessary for dust formation calculations are not available for lanthanoid elements. The second peak element of r-process is Xe, but the formation of Xe dust is difficult because it is a noble gas.

Table 1
Grain Species Considered in the Calculations

Grain Species	$\gamma/10^4$K	δ	a_0 (Å)	σ (erg cm^{-2})	$T_{\rm eq}$ (K)
C	8.640	18.974	1.281	1400	1800–2000
Fe	4.842	16.557	1.411	1800	1060–1180
Sr	1.456	7.067	2.364	165	430–500
Hf	7.390	16.220	1.745	1510	1630–1820
Pt	6.777	17.826	1.533	1770	1440–1600

Note. — The Gibbs free energy for the formation of clusters is approximated by $\Delta\mathring{g}/kT = -\gamma/T + \delta$, where the numerical values γ and δ are derived by least-squares fittings of the thermodynamics data (Chase, Jr. et al. 1985; Arblaster 2005) in the temperature range of T = 200–2500 K. The radius of the condensate per atom and the surface tension of the condensate are given as a_0 and σ, respectively (Elliott & Gleiser 1980; Nozawa et al. 2003). The equilibrium temperatures $T_{\rm eq}$ are presented for the density range of $n_i = 10^6$–10^8 cm^{-3}. See Nozawa & Kozasa (2013) for the details of the dust formation calculations.

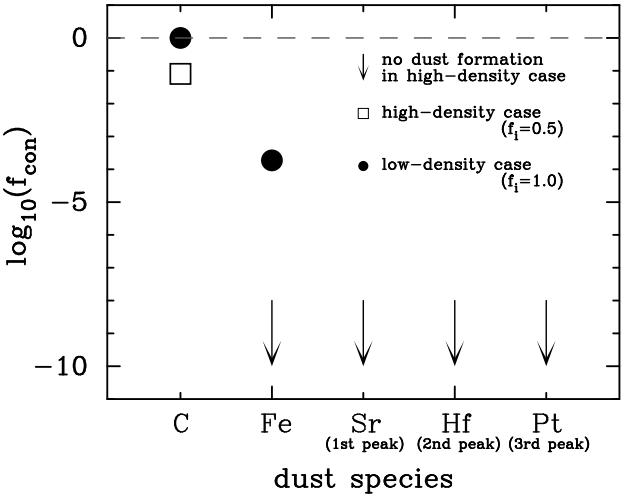

Figure 1. Condensation efficiency, which is defined as the mass fraction of atoms finally locked up in dust grains, of carbon, iron, strontium, hafnium, and platinum in the low-density (*square*) and high-density (*circle*) cases. The density of each element is $f_{\rm i}\rho$ where $f_{\rm i}$ = 1 (*filled*) or $f_{\rm i}$ = 0.5 (*open*) and ρ is given by equation (3).

in the case of efficient r-process nucleosynthesis. We conclude that the dust grains of heavy ($A_i \gtrsim 50$) elements are not expected to be formed in the low-density case. In particular, the condensation of r-process elements ($A_i \gtrsim 100$) is likely to be extremely difficult (see equation 5), unless the inhomogeneity of ejecta is taken into account.

In the high-density ejecta with inefficient r-process nucleosynthesis (κ = 0.1 cm^2 g^{-1}), the necessary condition of dust formation is relaxed. The results of dust formation are also shown in Figure 1. The condensation efficiency of carbon is unity for f_i = 1. Carbon grains form at $t \sim 7$ days. Despite the high density, the condensation efficiency of Fe grains is only $f_{\rm con} = 2\times10^{-4}$ even for f_i = 1 because of the low condensation temperature. Since Fe grains form much later than t_0 = 7 days[7], we exclusively focus on carbon for applications to GRB 130603B in the next subsection.

3.2. *Dust model for macronovae*

[7] Fe grains could form at earlier time in non-uniform ejecta, e.g., at the head of the ejecta where gas is rapidly cooled.

Figure 2 shows the condensation efficiency and average radius of carbon grains as a function of the isotropic equivalent mass of carbon $M_{\rm C}(4\pi/\Delta\Omega)$, where $M_{\rm C}$ is the mass of carbon available for dust formation. The density of ejecta is calculated as the isotropic equivalent mass divided by $4\pi R^3/3$. The condensation efficiency is unity above $M_{\rm C}(4\pi/\Delta\Omega) \sim 10^{-2}$, below which it decreases rapidly.

Once dust grains are formed in the ejecta, they absorb emission from the ejecta and emit photons with energies corresponding to their temperature. Assuming that dust emission is optically thin, we can choose the mass and temperature of dust so that its thermal emission explains the NIR emission of GRB 130603B. Figure 3 demonstrates one of the examples of a spectrum of the dust emission. For dust temperature of 1800 K, the mass of the required carbon grain is $M_{\rm d,C} \sim 8\times10^{-6}M_\odot$, which corresponds to $M_{\rm C} \sim 4\times10^{-3}M_\odot$ and $f_{\rm con} \sim 2\times10^{-3}$ for $\Delta\Omega = 4\pi$ (see Figure 2). Smaller the $\Delta\Omega$ is, larger the $f_{\rm con}$ is for a given $M_{\rm d,C} = (4\pi/\Delta\Omega) f_{\rm con} M_{\rm C}$. For instance, in the case of $(4\pi/\Delta\Omega) = 10$, $M_{\rm C} \sim 5\times10^{-4}M_\odot$ is required, which corresponds to $f_{\rm con} \sim 2\times10^{-2}$. Note that the required mass of carbon gas is consistent with the mass of ejecta which is shown in recent simulations, and that carbon grains do not evaporate because the dust temperature is lower than its evaporation (equilibrium) temperature. The opacity coefficient of the carbon grains is $\kappa_{\rm C} \sim 1.1\times10^4$ cm^2 g^{-1} at the J-band (1.2μm), which does not depend on their radius as long as the grain radius is much smaller than the wavelength. At 7 days in the rest frame, the absorption probability is above unity at wavelengths shorter than the J-band under the parameter choice : $(3M_{\rm d,C}/\Delta\Omega R^3)\kappa_{\rm C} R\beta \sim 0.7(4\pi/\Delta\Omega)(\lambda/1.2\,\mu{\rm m})^{-1.2}$. The absorption and emission coefficients are proportional to $\lambda^{-1.2}$ (Zubko et al. 1996). Thus, the dust grains absorb macronova emission and re-emit radiation in NIR bands.

Compared to a spectrum of the r-process model, which predicts a rather broad-line spectrum, the dust model provides an even more featureless spectrum. The spectrum of dust emission also deviates from a blackbody spectrum at wavelengths of $\gtrsim 5\mu$m because of the λ-dependence of the emission coefficient. Thus, a spectrum of the dust model can be observationally distinguished from both the r-process model and a pure blackbody spectrum.

Based on the discussion above, we can propose an alternative model for the NIR brightening of GRB 130603B, and generally NIR macronovae, which is schematically drawn in Figure 4. First, a macronova not powered by r-process elements happens (see Section 4 for possible heating sources). The low line opacity coefficient, e.g., $\kappa \sim 0.1$ cm^2 s^{-1}, makes this event bright in a blue band on timescale of a few day, as in the original work (Li & Paczyński 1998). Then, when the temperature of ejecta decreases to $\sim$ 2000 K, dust formation begins and the ejecta become opaque again by dust. The high opacity allows the macronova emission to heat dust grains, which emit absorbed photons in NIR bands. In other words, the observed NIR macronova can be the dust emission.

4. DISCUSSION AND SUMMARY

We have investigated dust formation in macronovae based on the temperature and density estimated from GRB 130603B. We have shown that dust of r-process elements hardly form even if they are abundantly produced. On the other hand, dust of light elements such as carbon can be

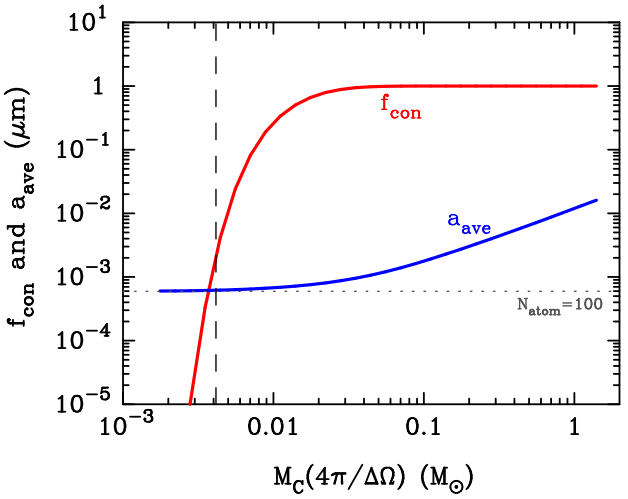

Figure 2. Condensation efficiency and average radius of newly formed carbon grains as a function of the isotropic mass of carbon $M_C(4\pi/\Delta\Omega)$ (M_C is the carbon mass available for dust formation). The radius of carbon grains with 100 atoms is also shown (*dotted*). The vertical dashed line marks the amount of carbon gas which is required to produce the dust emission spectrum ($M_{d,C} = 8 \times 10^{-6} M_\odot$) in Figure 3 for $\Delta\Omega = 4\pi$.

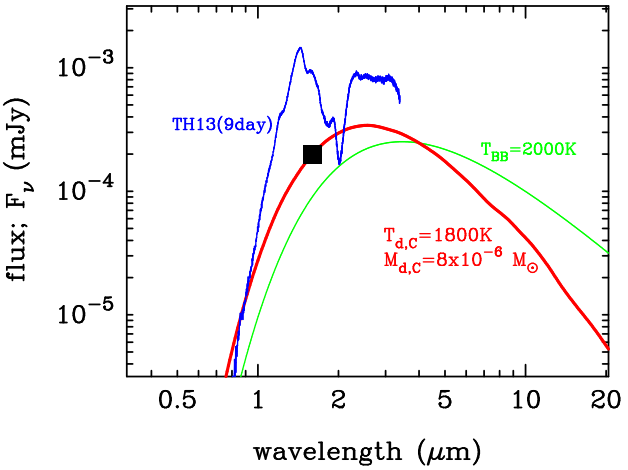

Figure 3. Thermal emission spectrum of carbon dust grains with 1800 K (*red*) in the observer frame. The black square is the observed flux of the NIR excess of GRB 130603B (Tanvir et al. 2013). For references, a spectrum of the r-process model (*blue*; Tanaka & Hotokezaka 2013, TH13) and a blackbody spectrum with $T = 2000$ K (*green*) are shown. The spectral shape of the dust emission is rather smooth than that of the r-process model. Note that the parameters of TH13 are not optimized for GRB 130603B.

formed. We have also suggested that the NIR macronova of GRB 130603B can be explained by the emission of light-element dust such as carbon grains. Thus, the dust model may be an alternative to the r-process model.

We inferred the temperature of ejecta from the observational result as $T_0 \sim 2000$ K. A heating source to realize this temperature may be the radioactive decay products of r-process elements. In r-process nucleosynthesis inefficient ejecta one possibility is the radioactive decay of heavy, but not r-process, elements (Barnes & Kasen 2013). Radioactive nuclei with the lifetime less than ~ 10 days release a significant fraction of radioactive energies and achieve $T \sim 2000$ K at ~ 7 days under a reasonable choice of ejecta mass. Another possibility is shock heating.

We should keep in mind that the discussions in this Letter are based on the observational result of GRB 130603B because this is the only existing sample. For instance, if

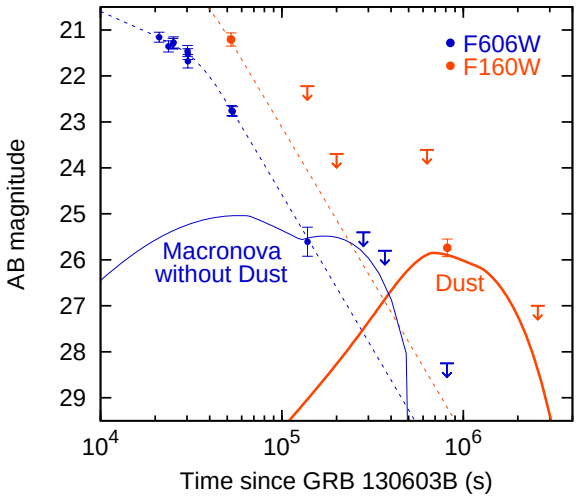

Figure 4. Schematic light curves for the dust interpretation of GRB 130603B. The data points are from Tanvir et al. (2013).

ejecta temperature is lower and density is much higher in another macronova, dust grains of r-process elements could be formed.

Our results have shown that newly formed grains are relatively small, consisting of ~ 100 up to $\sim 10^5$ atoms. We adopted the theory of Mie scattering in calculating the absorption coefficients of dust. However, they might deviate from the prediction of the theory for the dust only containing order-of-hundreds atoms.

We have considered homogeneous ejecta for simplicity. However, in reality, ejecta may be inhomogeneous, and dust may be formed in dense clumps, as discussed in supernovae (e.g., Kotak et al. 2009; Indebetouw et al. 2014). Larger dust grains may be formed in higher density clumps, and then opacity by dust can be changed by reflecting the spatial distribution of dust. Moreover, the consideration of the radial profile of ejecta may modify a dust formation history. Such effects are interesting to study in the future.

The dust model for NIR macronovae should be tested observationally. One is the confirmation of a featureless spectrum. As shown in Figure 3, a dust emission spectrum is even featureless compared to a broad spectrum in the r-process model. A spectrum in the dust model also deviates from a blackbody spectrum at long wavelengths. Another way is multi-wavelength observations of light curves from early epochs (see Figure 4). Without opacity of r-process elements, a macronova is bright and blue in an early phase. It becomes red later by the emission of newly formed dust. In both cases, quick follow-up observations are important to understand the origin of NIR macronovae as well as the nucleosynthesis in the mergers of compact stellar objects.

We thank N. R. Tanvir for clarifying parameter definitions in the paper of his team, thank M. Tanaka for providing us with the numerical data of a macronova spectrum (Figure 3), and thank T. Hotokezaka, T. Nakamura, Y. Sekiguchi, and M. Shibata for discussions. T. Nakamura had been also investigated dust formation in macronova independently of us. This work is supported by JSPS KAKENHI 24·9375 (H. T.), 22684004, 23224004 (T. N.), 24000004, and 22244030 (K. I.), by MEXT KAKENHI 24103006 (K. I.), and by World Premier International Research Center Initia-

tive (WPI Initiative), MEXT, Japan.

REFERENCES

Abadie, J., & LIGO Collaboration. 2010, Nucl. Instrum. Methods Phys. Res. Sect. A, 624, 223
Accadia, T., et al. 2011, Class. Quantum Grav., 28, 114002
Arblaster, J. W. 2005, Platinum. Metals. Rev., 49, 141
Barnes, J., & Kasen, D. 2013, ApJ, 775, 18
Bauswein, A., Goriely, S., & Janka, H.-T. 2013, ApJ, 773, 78
Berger, E., Fong, W., & Chornock, R. 2013, ApJ, 774, L23
Chase, Jr., M. W., Davies, C. A., Downey, Jr., J. R., Frurip, D. J., McDonald, R. A., & Syverud, A. N. 1985, J. Phys. Chem. Ref. Data Suppl., 14, 1
Dessart, L., Ott, C. D., Burrows, A., Rosswog, S., & Livne, E. 2009, ApJ, 690, 1681
Elliott, J. F., & Gleiser, M. 1980, Thermochemistry for Steelmaking, Vol. 1 (Addision-Wesley)
Fernández, R., & Metzger, B. D. 2013, MNRAS, 435, 502
Goriely, S., Bauswein, A., & Janka, H.-T. 2011, ApJ, 738, L32
Hotokezaka, K., Kiuchi, K., Kyutoku, K., Okawa, H., Sekiguchi, Y.-i., Shibata, M., & Taniguchi, K. 2013a, Phys. Rev. D, 87, 024001
Hotokezaka, K., Kyutoku, K., Tanaka, M., Kiuchi, K., Sekiguchi, Y., Shibata, M., & Wanajo, S. 2013b, ApJ, 778, L16
Indebetouw, R., et al. 2014, ApJ, 782, L2
Jin, Z.-P., Xu, D., Fan, Y.-Z., Wu, X.-F., & Wei, D.-M. 2013, ApJ, 775, L19
Kasen, D., Badnell, N. R., & Barnes, J. 2013, ApJ, 774, 25
Korobkin, O., Rosswog, S., Arcones, A., & Winteler, C. 2012, MNRAS, 426, 1940
Kotak, R., et al. 2009, ApJ, 704, 306
Kulkarni, S. R. 2005, arXiv:astro-ph/0510256
Kuroda, K., & LCGT Collaboration. 2010, Class. Quantum Grav., 27, 084004
Kyutoku, K., Ioka, K., & Shibata, M. 2013, Phys. Rev. D, 88, 041503
—. 2014, MNRAS, 437, L6
Li, L.-X., & Paczyński, B. 1998, ApJ, 507, L59
LIGO Scientific Collaboration et al. 2013, arXiv:1304.0670
Metzger, B. D., & Fernández, R. 2014, arXiv:1402.4803
Metzger, B. D., et al. 2010, MNRAS, 406, 2650
Nakar, E., & Piran, T. 2011, Nature, 478, 82
Nozawa, T., & Kozasa, T. 2013, ApJ, 776, 24
Nozawa, T., Kozasa, T., Umeda, H., Maeda, K., & Nomoto, K. 2003, ApJ, 598, 785
Pinto, P. A., & Eastman, R. G. 2000, ApJ, 530, 757
Piran, T., Nakar, E., & Rosswog, S. 2013, MNRAS, 430, 2121
Rosswog, S., Korobkin, O., Arcones, A., & Thielemann, F.-K. 2013, arXiv:1307.2939
Rosswog, S., Liebendörfer, M., Thielemann, F.-K., Davies, M. B., Benz, W., & Piran, T. 1999, A&A, 341, 499
Rosswog, S., Ramirez-Ruiz, E., & Davies, M. B. 2003, MNRAS, 345, 1077
Ruffert, M., & Janka, H.-T. 2001, A&A, 380, 544
Ruffert, M., Janka, H.-T., Takahashi, K., & Schaefer, G. 1997, A&A, 319, 122
Shibata, M., Suwa, Y., Kiuchi, K., & Ioka, K. 2011, ApJ, 734, L36
Surman, R., Caballero, O. L., McLaughlin, G. C., Just, O., & Janka, H.-T. 2013, arXiv:1312.1199
Takami, H., Kyutoku, K., & Ioka, K. 2013, arXiv:1307.6805
Tanaka, M., & Hotokezaka, K. 2013, ApJ, 775, 113
Tanaka, M., Hotokezaka, K., Kyutoku, K., Wanajo, S., Kiuchi, K., Sekiguchi, Y., & Shibata, M. 2014, ApJ, 780, 31
Tanvir, N. R., Levan, A. J., Fruchter, A. S., Hjorth, J., Hounsell, R. A., Wiersema, K., & Tunnicliffe, R. L. 2013, Nature, 500, 547
Wanajo, S., Sekiguchi, Y., Nishimura, N., Kiuchi, K., Kyutoku, K., & Shibata, M. 2014, arXiv:1402.7317
Zubko, V. G., Mennella, V., Colangeli, L., & Bussoletti, E., 1996, MNRAS, 282, 1321